16TH EUROPEAN CONFERENCE ON EARTHQUAKE ENGINEERING THESSALONIKI 18 - 21 JUNE 2018

TOWARDS RAPID PREDICTION OF TOPOGRAPHIC AMPLIFICATION AT SMALL SCALES: CONTRIBUTION OF THE FSC PROXY AND PLEIADES TERRAIN MODELS FOR THE 2016 AMATRICE EARTHQUAKE (ITALY, MW 6.0)

Emeline MAUFROY[1], Pascal LACROIX[2], Emmanuel CHALJUB[3], Christophe SIRA[4], Gerardo GRELLE[5], Laura BONITO[6], Mathieu CAUSSE[7], Víctor M. CRUZ-ATIENZA[8], Fabrice HOLLENDER[9], Fabrice COTTON[10], Pierre-Yves BARD[11]

ABSTRACT

Destructive earthquakes occurring over mountainous regions regularly question the role of surface topography on the spatial distribution of damages. This is the case of the recent Amatrice M_W 6.0 earthquake (Italy, August 24th 2016), which caused nearly 300 fatalities and severe, spatially variable, structural damages in ancient villages located in areas of pronounced topography.

Understanding the near-field damage distribution requires to unravel the contributions of variable physical vulnerability and input ground motion. As a first step towards this goal, we compare the damage information provided at metric scale by the Copernicus European program to the so-called Frequency-Scaled Curvature (FSC) proxy for topographical seismic amplification. We apply the FSC proxy to high-resolution (2 m) DSM provided by Pléiades satellite imagery and further investigate the correlations between the predicted amplification and the distribution of damages in the most affected village (Amatrice).

We find a striking spatial correlation between the locations of greatest structural damages and of largest topographic amplification. However, since the damaged areas also correspond to the locations of the most vulnerable buildings, it is still difficult to call for a causal link between topography and damages. Yet, our results suggest that the settlement of ancient villages in mountainous regions like the Apennines results in systematic higher levels of seismic hazard because of what we call the "promontory effect".

We further discuss the application of our method to rapid, high-resolution forecast of earthquake ground motion and damages in mountainous areas.

Keywords: Topographic site effect; Ground-motion proxy; Ground-motion prediction; Amatrice earthquake; earthquake damages.

1. INTRODUCTION

Local site conditions, that is, the local geology and geometry of the surface, can significantly affect seismic ground motions in the frequency range where most buildings are vulnerable (generally above 1 Hz). Increasing attention is therefore paid to include site conditions in microzonation studies to assess

[1]Associate professor, Univ. Grenoble Alpes CNRS/IRD/IFSTTAR ISTerre, France, emeline.maufroy@univ-grenoble-alpes.fr
[2]Associate professor, Univ. Grenoble Alpes CNRS/IRD/IFSTTAR ISTerre, France, pascal.lacroix@univ-grenoble-alpes.fr
[3]Associate professor, Univ. Grenoble Alpes CNRS/IRD/IFSTTAR ISTerre, France, emmanuel.chaljub@univ-grenoble-alpes.fr
[4]Engineer, French Central Seismological Office (BCSF), Univ. of Strasbourg, EOST, France, christophe.sira@unistra.fr
[5]Researcher, Department of Civil and Environmental Engineering, Sapienza Univ. of Rome, Italy, gerardo.grelle@uniroma1.it
[6]PhD student, Department of Science and Technology, Univ. of Sannio, Benevento, Italy, laura.bonito@unisannio.it
[7]Associate professor, Univ. Grenoble Alpes CNRS/IRD/IFSTTAR ISTerre, France, mathieu.causse@univ-grenoble-alpes.fr
[8]Associate professor, Departamento de Sismología, Instituto de Geofísica, UNAM, Mexico, cruz@geofisica.unam.mx
[9]Researcher, CEA, French Alternative Energies and Atomic Energy Commission, DEN, France, fabrice.hollender@cea.fr
[10]Professor, GFZ German Research Centre for Geosciences, Potsdam, Germany, fcotton@gfz-potsdam.de
[11]Professor, Univ. Grenoble Alpes CNRS/IRD/IFSTTAR ISTerre, France, pierre-yves.bard@univ-grenoble-alpes.fr

seismic hazard. Although seismic amplification induced by the geometrical focusing effect of the topography was shown to be significantly lower than the one due to strong impedance contrasts in the near surface (Assimaki et al. 2005; Maufroy et al. 2012), its study has been revived because, for some destructive earthquakes, the topography strikingly correlates with the distribution of damages (Kawase & Aki 1990; Spudich et al. 1996; Assimaki et al. 2005; Hough et al. 2010; Pischiutta et al. 2010). A long-term debate exists about the explanation for such observations. Depending on the authors, the importance of the contribution of surface geometry to earthquake damages varies from negligible (Burjánek et al. 2014) to weak (Pischiutta et al. 2010) and even significant (Buech et al. 2010).

Several reasons make the quantification of the topographic site effect particularly difficult. First, it is not easily observable because it requires deploying dense instrumentation over sharp topography, and it does not necessarily produce narrow and clear peaks of amplified frequencies like resonance do. Second, its estimation by numerical simulation often underestimates the three-dimensional fractal dimension of surface topography and is therefore often limited to smooth, unrealistic geometries. Finally, surface topography amplifies the ground motion in the same frequency range as lithological or environmental (fracturing, saturation, alteration) effects, which makes it challenging to be isolated on the field. Because of those difficulties, it was considered that no single or simple proxy could capture the characteristics of the topographic site effect (Hough et al. 2010).

Yet, recent developments based either on the analysis of synthetic datasets (Maufroy et al. 2015a; Rai et al. 2016) or on automated terrain-classification methods (Burjánek et al. 2014; Grelle et al. 2016, 2017; Rai et al. 2017) provide interesting tools that enable the estimation of topographic site effects at high resolution over large areas. For example, Maufroy et al. (2015a), after analyzing a comprehensive set of numerical simulations, identified the curvature of the surface as the geometric parameter controlling the topographic amplification of seismic waves. They obtained a linear correlation between surface curvature and the most amplified *S*-wavelength given by the results of the numerical simulations, from which they derived the so-called Frequency-Scaled Curvature (FSC) proxy for topographic seismic amplification. The FSC proxy provides a continuous frequency-dependent function, which only requires information about the surface geometry provided by a DSM (Digital Surface Model) or DTM (Digital Terrain Model). The mapping of the FSC amplification over DSM/DTM provides a new way for illustrating the contribution of topographic site effects to the spatial variability of earthquake ground motion and its possible relation to earthquake damages (Maufroy et al. 2015a).

The Amatrice earthquake (Italy, Mw 6.0) occurred in the Central Apennines on August 24th, 2016, at 01:36:32 UTC. It strongly affected a rural area that includes several small towns, Mediterranean-style villages where buildings are gathered in small spaces, causing nearly 300 fatalities. In that near-source area (under 12 km of epicentral distance), the effects of the earthquake were highly variable: the villages were differently affected, from destroyed to slightly damaged (though they could be further damaged by the next earthquakes of the sequence, including the strongest event, Mw 6.5, on October 30th, 2016). Inside the largest village (i.e., Amatrice, which gave its name to the first event of the sequence), the damages appear highly variable down to the hectometric scale (Fiorentino et al. 2017). The damages vary even down to the decametric scale for smaller villages (e.g., Pescara del Tronto). All the places strongly affected by the Amatrice earthquake have (at least) one common point: they are old villages. The vulnerability of ancient constructions therefore plays a key role in the spatial variability of the damages inside the epicentral area. But another common point is apparent: the damaged areas are all located over topographies, as the earthquake occurred in the mountainous zone of the Apennines. Many ancient villages in the area are indeed placed over ridges or hills that are more or less accentuated.

Through the FSC proxy computed at small scales on DSM provided at high-resolution (2 m) by Pléiades satellite imagery, we investigate the correlation between topographic curvature and seismic damages for the Amatrice earthquake. The damage information is provided at metric scale by the Copernicus European program shortly after the earthquake (1 or 2 days later). We question if, despite the clear dominant role played by the vulnerability of the structures, it remains possible to distinguish any effect of the topography over the spatial variability of the damages. We investigate the most-affected village of Amatrice and relate the surface curvature with various ranges of affected *S*-wavelengths, emphasizing the level of FSC topographic amplification reached at different spatial scales.

Then, we discuss the prerequisites to perform such case study within the scope of rapid applications for future earthquakes in mountainous areas. In particular, we quantify the necessary DSM/DTM resolution to reach the smallest scales involved (in this case, decametric), and we emphasize the need to correct

for buildings and forests in satellite DSM to obtain DTM including only terrain topography.

2. THE FSC PROXY FOR TOPOGRAPHICAL SEISMIC AMPLIFICATION

The FSC proxy predicts the topographic-amplification function at any point of a given topographic model, based on the surface curvature, that is, the second derivative of the surface elevation. This proxy was elaborated from the frequency-dependent linear correlation found between topographic amplification as computed by 3D numerical simulations of the earthquake ground motion and the surface curvature, as summarized in Figure 1. Its elaboration is fully described in Maufroy et al. (2015a).

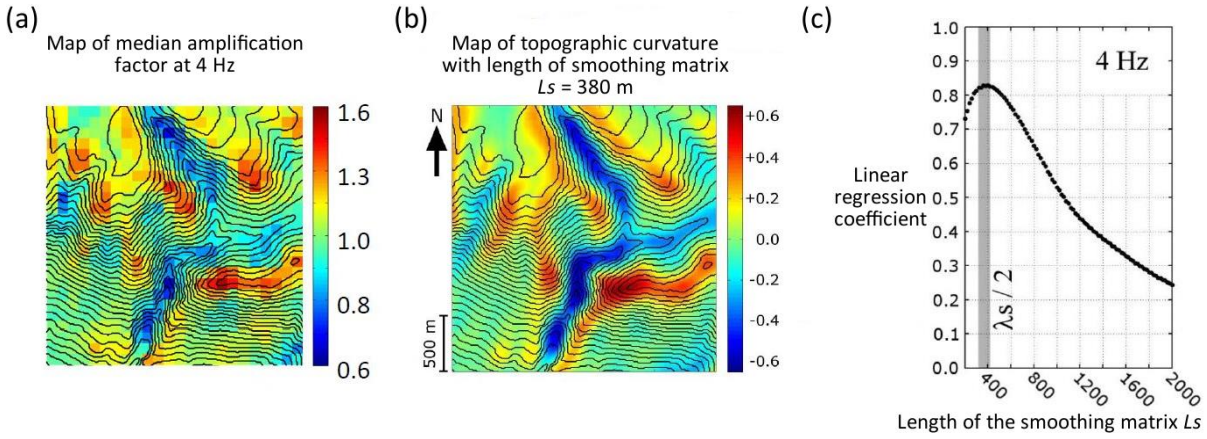

Figure 1. Example of the linear correlation obtained between (a) median topographic amplification factor (as measured by MRM – see Maufroy et al. 2012) and (b) smoothed curvature. Those values are mapped over the digital model of the real topography around the French LSBB Underground Laboratory (elevation contour lines every 20 m), which was used in the study by Maufroy et al. (2015a). This correlation, here shown at 4 Hz only, is at the base of the FSC proxy. To be obtained, values at (a) required 200 3D finite-differences simulations of earthquake ground motion performed on national high-performance computers, while values at (b) only required a few minutes of calculation on a regular computer. The linear correlation is maximized when (c) the length L_S of the unit matrix used to smooth the topographic curvature is equal to the *S*-wavelength λ_S divided by 2. Readers are referred to Maufroy et al. (2015a) for further details on the elaboration of the FSC proxy.

The FSC proxy was derived from a bank of 115200 seismic waveforms obtained by 3D finite-difference simulations in homogeneous media with realistic 3D topography (Maufroy et al. 2012). The proxy is elaborated to predict the amplification factor as a function of the *S*-wavelength, and thus can be converted into a function of frequency if the *S*-velocity of the subsurface is known. Because its computation is costless, the FSC proxy can be mapped for any *S*-wavelength or for a given, possibly large range of *S*-wavelengths. This allows for investigating the effect of the surface geometry on earthquake ground motion at many different scales. The obtained FSC amplification function allows determining the level of topographic amplification (or deamplification) and the value (or the range) of the most-amplified *S*-wavelength(s), at any point of the topographic surface.
The main equation defining the FSC proxy is (see Equation 6 in Maufroy et al. 2015a):

$$\mathrm{MAF}(f) = (0.0008 \times \lambda_S) \times C_S(L_S) + 1 \qquad (1)$$

where MAF is the median amplification factor at frequency f, λ_S is the related *S*-wavelength, and $C_S(L_S)$ is the surface curvature smoothed over the length L_S, which is defined as half the seismic *S*-wavelength. A few remarks can be made from this simple equation.
First, the effect of surface topography on earthquake ground motions is known to be source-dependent, this is why the FSC proxy at a site is related to the "median" amplification factor, that is, to the median value of the distribution of amplification factors obtained for a large range of hypocenter locations around the site. The variability of the amplification factor distribution (the median absolute deviation) is potentially quite large and can also be quantified by the FSC proxy (see Equations 7 and 8 in Maufroy

et al. 2015a, which approximate the upper 84th and lower 16th percentiles of the distribution, respectively). In this study, we focus on the median value of the FSC proxy, but it should be kept in mind that if the actual source location allows for a strong (resp. weak) coupling between the incoming wavefield and the local surface topography, then the median value would under- (resp. over-) estimate the actual amplification factor.
Second, in order to optimize the wavelength-dependent linear correlation between the smoothed curvature C_S and the topographic amplification, the value of the smoothing length L_S is defined as:

$$\lambda_S = 2\ L_S = 4 \times n \times h \tag{2}$$

where n is the size (in pixel) of the boxcar unit matrix used to smooth the surface curvature, and h is the resolution of the topographic model in meter. Therefore, the spatial resolution has an impact on the computation of the FSC proxy: it controls the minimal S-wavelength (or highest frequency) that can be investigated. The parameter n has to be an odd number equal to or greater than 3. This implies that the minimal L_S equals $6 \times h$ and that the minimal λ_S equals $12 \times h$. Table 1 indicates the minimal λ_S reached with different resolutions of the topographic model, followed by the allowed step in meter between two consecutive investigated S-wavelengths (due to n being an odd number). Of course, the higher the resolution of the topographic model, the higher the frequencies reached by the FSC proxy. Currently, free terrain data are available at a resolution of 30 m everywhere on the planet, which allows investigating the topographic site effect for S-wavelengths as small as 360 m (the second smallest λ_S being 600 m). For cases where the topographic features are small or much intricate, a higher resolution is required. In the present study, where the investigated city and the corresponding damages have an extent not greater than the hectometric scale, a high-resolution topographic model is mandatory.

Table 1. Minimal S-wavelength (λ_S min) that can be investigated by the FSC proxy as a function of the topographic-model resolution h, followed by the allowed step between two investigated S-wavelengths (λ_S step).

Topo. resolution (h)	**λ_S min (12 h)**	**λ_S step (8 h)**
2 m	24 m	every 16 m
10 m	120 m	every 80 m
30 m	360 m	every 240 m
100 m	1200 m	every 800 m

Third, it must be considered that the FSC amplification factors are not related to a reference site, but to a reference level defined by the Median Reference Method (MRM, as described in Maufroy et al. 2012). Herein, the reference level is defined by the median ground motion recorded or simulated over the area of interest; if concave valleys, slopes and convex ridges are equally instrumented in this area, the reference level is spatially located where the surface curvature equals 0, i.e., on flat terrain or at mid-slope (where concave slopes become convex). The spatial location of the reference level can vary with the considered frequency range, and thus corresponds to different topographic features at different scales. It advantageously avoids the choice of a unique reference site. But it cannot coincide with the typical reference site taken at the foot of the hill, which always corresponds to a zone of deamplification in the MRM (negative curvature). Thus, FSC amplification factors are intrinsically low factors, but they allow for estimating deamplification (due to de-focalization of seismic waves by the concave geometry of valleys), which can be as strong as amplification. Stolte et al. (2017) recently illustrated the differences in amplification level reached by different methods to estimate topographical site-effects: Figure 8 in their study shows how the MRM produces amplification factors that are systematically lower than those of other methods, such as the classical Standard Spectral Ratios using a reference station at the foot of the hill. Their same figure also shows that only the MRM is able to estimate the deamplified peak in valleys affected by adjacent topography. If the aim of a given study is to derive crest/valley factors, those can be simply retrieved from FSC amplification factors by dividing the FSC estimation at the crests by the FSC estimation at the foothills. Following this process, one obtains amplification factors equivalent to those of the MRM_V as defined by Stolte et al. (2017). Concerning the present study, as one

goal is to assess the spatial variability of the topographic site effect, all the FSC factors are given relative to the MRM referential, which allows estimating both amplification and deamplification effects.
Finally, note that the FSC amplification factors apply to the arithmetic mean of the horizontal components of the ground motion. The proxy is therefore not able to discriminate whether one horizontal component is more amplified than the other (although it is a common feature of the topographic site effect, due to preferential polarization of the seismic waves at the top of elongated ridges).
All the previously discussed aspects imply that the FSC amplification is a rather smooth function of frequency. The obtained peaks are not narrow; the predicted amplification may even be broadband over a large range of affected *S*-wavelengths (some examples can be found in Maufroy et al. 2015a, 2015b).

3. TOPOGRAPHY AND DAMAGE INFORMATION AT AMATRICE

3.1 Pléiades high-resolution DSM

To retrieve the topography in Amatrice region, we use a tri-stereo acquisition of Pléiades satellite images taken on October 29th, 2016, after the Amatrice earthquake, over an area of 844 km². This allows computing a high-resolution Digital Surface Model (DSM), as shown on Figure 2. Advantageously, this DSM has a resolution of 2 m and covers a large part of the epicentral area. One disadvantage is that we do not obtain a terrain model, so vegetation and buildings are included in the DSM. Concerning the methodology, the tri-stereo acquisition is very much suitable to reduce the gaps of the DSM in steep and mountainous areas. We use the free software Ames Stereo Pipeline (Shean et al. 2016), and the methodology developed in Lacroix (2016) to generate the DSM. A coarse DSM is first computed with a resolution of 30 m, before map-projecting the two images on it. Parallaxes between the two map-projected images are again estimated to refine the coarse DSM down to 2 m. Uncertainties of such Pléiades DSM is about 0.7 m on flat areas, increasing with slopes (Berthier et al. 2014; Lacroix et al. 2015).

3.2 Damages effects at metric scale by Copernicus

A rapid estimation of the damages is given a few days after a significant earthquake by the European program Copernicus from remote satellite imagery. The produced grading maps provide an instant snapshot of the damages, which remains available even if the cities are later further affected by following earthquakes in the seismic sequence. For the Amatrice earthquake, the program produced high-resolution images and vector data characterizing the damage pattern at metric scale. Those remote estimations are not exempted of uncertainty, as, for example, damage may be under-estimated when the roof is not collapsed (Fiorentino et al. 2017). Still they are much valuable for their high resolution and quick availability.
The hypocenter of the 2016 Amatrice earthquake was located at 8 km depth below Accumoli village. The moment tensor solution shows normal faulting with planes striking along the Apennines (Tinti et al. 2016). More than ten small towns were damaged by this earthquake, among the most devastated: Accumoli (1 km of epicentral distance, 11 fatalities that occurred in the main village and in the neighborhoods), Amatrice (9 km of epicentral distance, 234 fatalities), Arquata Del Tronto (11 km of epicentral distance, 49 fatalities, mostly in the "frazione" Pescara Del Tronto at 7 km of epicentral distance). High values of peak ground acceleration were indeed observed closed to Amatrice (0.92 g on the EW component at AMT station of the Italian Accelerometric Network; Pischiutta et al. 2016). Modeling of the rupture history of the main shock and strong ground-motion analyses show directivity effects occurring mainly NW from the hypocenter, but also SE towards Amatrice (located in the backward sector) because of a bilateral rupture (Pischiutta et al. 2016; Tinti et al. 2016). The ground-motion spatial variability at large scales (kilometric scale and above) is rather well explained by source effects, as shown by those studies. However, below the kilometric scale, the effects of the earthquake remain highly variable in the near source: many villages in the epicentral area (under 12 km of epicentral distance) were differently affected, from destroyed to lightly damaged. Over Amatrice, the Copernicus grading map indicates that the village suffered two different levels of damage on the hectometric scale: the ancient part of the village, including old and highly vulnerable buildings, was largely destroyed,

while the modern part was less affected.

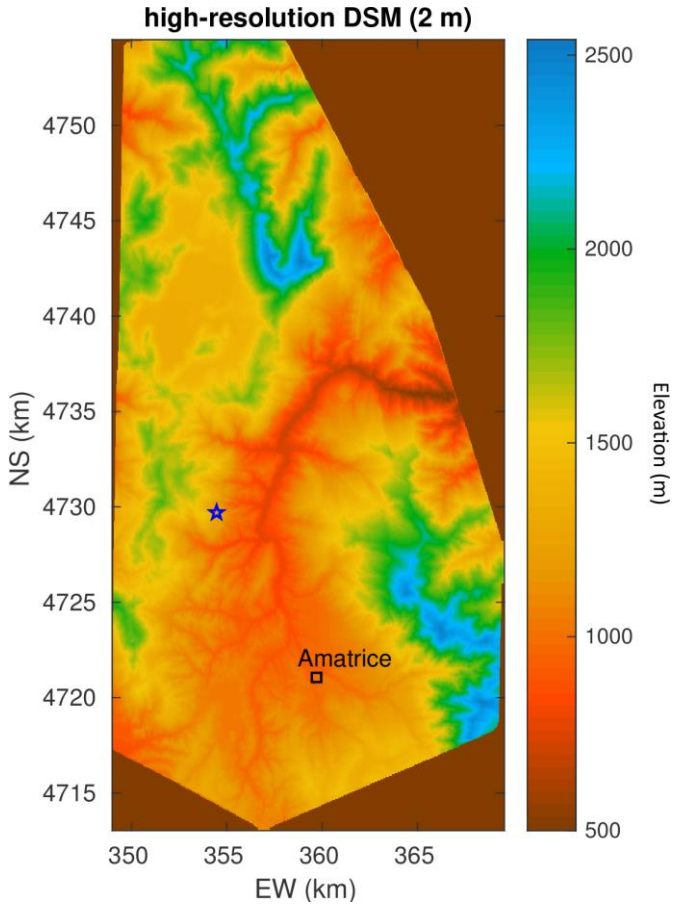

Figure 2. Digital surface model of the Amatrice region obtained from Pléiades satellite imagery. Resolution of DSM is 2 m. The coordinates correspond to the geodetic system WGS 84 with UTM projection. The blue star locates the epicenter of the Amatrice earthquake, and the black square indicates the place of Amatrice city.

4. FSC TOPOGRAPHIC AMPLIFICATION VS. DAMAGES: CASE STUDY OF AMATRICE

We apply the FSC proxy to the high-resolution DSM provided by Pléiades satellite imagery, and compare the results obtained over Amatrice village with the pattern of damages provided by the Copernicus program. Figure 3 shows a summary of this comparison exercise. Before analyzing those results in details, two remarks on the FSC computation are useful:

(1) As the velocity structure in Amatrice hill is poorly known, we choose to analyze the amplification as a function of *S*-wavelength instead of frequency. Although it is not usual, this prevents any misinterpretation that could be due to that poor knowledge in the near-surface velocities. We also believe that a study related to wavelength is appropriate to investigate which spatial scales in the topography are involved in the seismic topographic amplification. Once the velocity structure inside Amatrice hill is known and if this structure is not heterogeneous at the scale of the involved λ_S, the results presented in this study would be easily converted into frequencies.

(2) The FSC proxy allows computing the topographic-amplification function at every point of the DSM, i.e., every 2 m in space. Additionally, due to the high-resolution in the surface topography, the lowest investigated λ_S is equal to 24 m. The results are therefore quite numerous both in space and in wavelength. First, we choose to restrict the results presented in this study to an area of 1 km² centered on Amatrice hill. Second, we show results only for *S*-wavelengths greater than 200 m, this choice being discussed after the presentation of the results.

Figure 3 compares the results of the FSC proxy applied over Amatrice hill (left) with the damages estimation by Copernicus (right). For the sake of clarity, both information are provided in map. Particularly, the map on Figure 3a shows the maximum of the median FSC amplification function (i.e., of the 50th percentile of the distribution predicted by the proxy) reached over λ_S ranging ~300-1000 m. The area that was most-damaged in Amatrice is indicated on Figure 3b by the cyan contour line, which is also reported on the FSC map to help visual comparison. The Copernicus grading map clearly illustrates the different levels of damage that separate the city in two distinct halves: the highest damages with most destructions are located in the NW ancient part of the city, while the SE modern part is clearly less affected. This is the immediate impact of the differences in vulnerability of the structures.
However, we also find a striking spatial correlation between the locations of the greatest structural damages and the largest topographic amplification as predicted by FSC. Figure 3a shows that, in the considered λ_S range, the highest FSC amplification factors are located in the NW part of the hill, while the SE part is less, or even not, affected by topographic amplification. Indeed the NW part is surrounded by steep slopes, which participate in the geometric focusing of the seismic waves at the hilltop or at the crests. On the contrary, the SE part of the hill is larger, rather flat and surrounded by smoother slopes. Consequently, we observe a spatial variability in the FSC topographic amplification that correlates very well with (1) the spatial variability of the damages, but also with (2) the pattern of the structural vulnerability. Due to this double correlation, the link between damage and topographic amplification remains to some extent elusive. Indeed, many other factors impact the behavior of buildings under seismic solicitation, such as their vulnerability and dimensions, the local soil conditions, the frequency content of the input seismic motion, to name but a few.

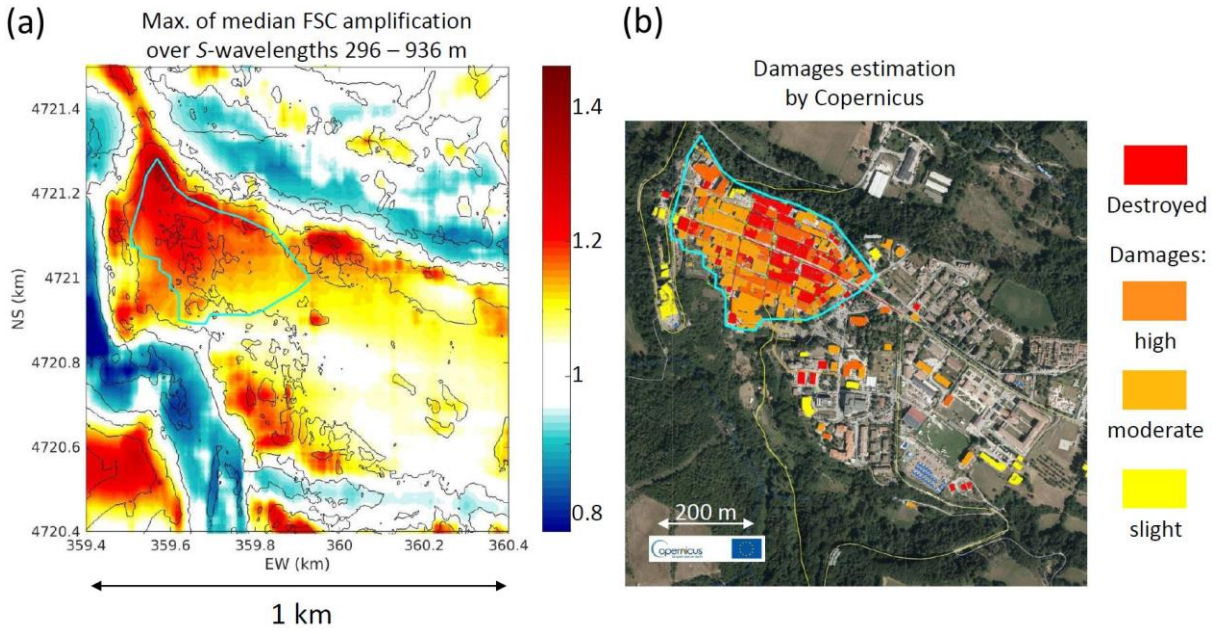

Figure 3. Comparison of (a) the prediction given by the FSC proxy of topographic amplification over Amatrice city with (b) the Copernicus grading map on the same area after the Amatrice earthquake. Results on (a) are represented as the map of the maximum FSC median amplification factor (color scale) reached over short *S*-wavelengths ranging 296-936 m, and superimposed to elevation contour lines every 20 m. The Copernicus Emergency Management Service published the map shown on (b) on August 31, 2016, displaying the situation as of August 25, 2016. The cyan contour line designates on both maps the location of the most-damaged part of the city.

Independently of this first observation, our mapping of the FSC amplification over the topography in Amatrice area clearly illustrates that the topographic site effect has a strong control on the spatial variability of the earthquake ground motion. Figure 4 shows how the FSC map varies when considering three different *S*-wavelength ranges: (1) for λ_S larger than those considered on Figure 3a; (2) for short λ_S ranging ~400-900 m; and (c) for very short λ_S ranging ~230-380 m. Depending on the considered λ_S, the FSC map can appear quite different. It is noteworthy that the maximum FSC topographic amplification

is always located in the most-curved topographic areas, but that notion of curvature is strongly scale-dependent, hence wavelength-dependent.
A remarkable feature is the shortest distance separating amplified and deamplified areas. This distance can be as short as 100 m over Amatrice area. As described in Section 2, FSC factors are characteristically low factors (we quickly recall the three reasons here: median values of a highly variable distribution, arithmetic mean of the horizontal components of the ground motion, and reference level defined at mid-slope where curvature is null). In our case study, we observe a FSC factor up to 1.9 between amplified/deamplified zones separated by only 100 m, which we interpret as a quite strong spatial variability of the seismic ground motion over Amatrice, obtained by considering only the topography.

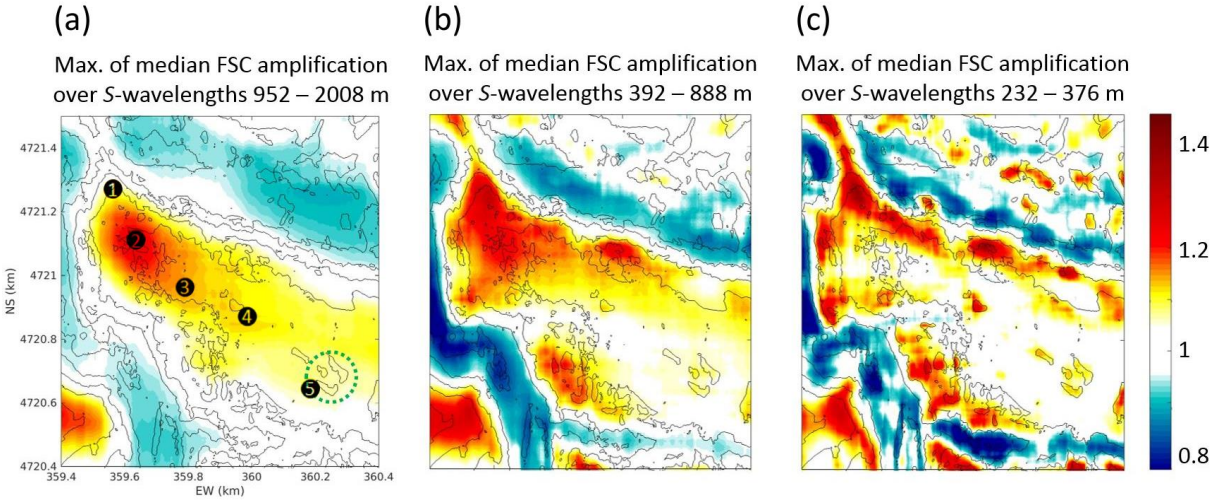

Figure 4. Maps of FSC topographic amplification over Amatrice city for three different *S*-wavelength ranges: (a) long λ_S (952-2008 m), (b) short λ_S (392-888 m), and (c) very short λ_S (232-376 m). The represented values are the maximum factor reached in the considered wavelength range at the 50th percentile (*i.e.*, at the median) of the amplification distribution predicted by the FSC proxy. Single-point amplification functions are extracted at the five sites indicated on (a) and are shown in Figure 5. The dotted green circle points the location of a large building clearly observable in the DSM and that locally affects the FSC results. Elevation contour lines are every 20 m.

That spatial variability is also observable in Figure 5, which shows individual-site FSC amplification functions extracted at 5 sites whose locations are indicated in Figure 4a. Those sites are aligned on a NW-SE axis, along the direction of elongation of Amatrice hill. They are separated by a distance of 200 m (± 50 m). The topographic amplification clearly decreases from a maximum observed at NW (site 1) to a minimum at SE (site 5). We also observe a progressive shift in the most-amplified wavelengths. Site 1 shows a clear peak centered at λ_S = 350 m and no amplification for λ_S larger than 1500 m; the center of peak at site 2 (located 160 m southeastward from site 1) shifts at λ_S = 1000 m. In frequency, this would translate by topographic amplification in higher frequencies at the NW promontory compared to the amplification at the center of the damaged area. The three other sites are affected by some moderate amplification only for λ_S larger than 1000 m.

Overall, Figures 4 and 5 indicate that the ground-motion spatial variability due to topography occurs in the same small scales (decametric to hectometric) than the spatial variability observed in the damages. This study shows that the small scales are now reachable for site-effect analyses, thanks to newly available information at high resolution, and that reaching those scales are essential for investigating the origins of earthquake damages.

5. CONTRIBUTION OF OUR METHOD TO RAPID, HIGH-RESOLUTION FORECAST OF DAMAGES IN MOUNTAINOUS AREAS

The simplicity of our method makes it an interesting option for a variety of applications to predict the earthquake ground motion in mountainous areas. For example, the FSC proxy could be easily inserted in GMPEs (provided they are formulated in Fourier domain; though the bank of synthetic waveforms described in Section 2 could also be used to derive a proxy for response spectra), or in Shake Maps. The validation of the FSC proxy on real observations is an on-going and long-term task, to which the present study on Amatrice participates (a few other examples are given in Maufroy et al. 2015b). The only caution we issue is that taking into account the focusing effect of topography in any prediction (and whatever is the chosen proxy) should be completed by a prediction of the effects of near-surface geology (resonance effects, for instance). Any prediction considering only the geometry of the free surface is by definition always unrealistic, despite the positive results shown in the present study.

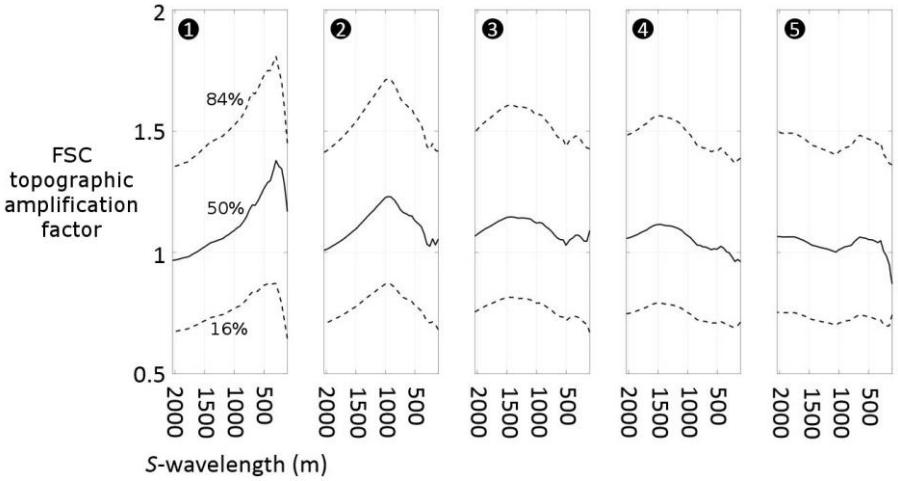

Figure 5. FSC amplification functions related to *S*-wavelength at five single sites, whose locations are indicated on Figure 4a. At each site, the distribution of amplification factors predicted by the FSC proxy for a full coverage of source back azimuths is represented by its median (solid line) and by the upper (84%) and lower (16%) percentiles (dashed lines).

Another perspective concerns the rapid forecast of ground motion and/or damages at high-resolution mapping. The "rapid" and "mapping" aspects imply the use of proxies that are both costless and accurate, and we believe the FSC proxy is appropriate for that purpose. The computation and mapping of the FSC amplification over a DTM at standard resolution (10-30 m) can be performed over a personal computer. For the present study, the use of a DSM at high resolution required more computational power, but which remains much accessible. We performed the FSC computation using a Matlab script (with no particular optimization of the algorithm for the calculation of the smoothed curvature). This script required for running about 20 Go RAM during 10 min (only one processor) to get the results over an area of 9 km² at a resolution of 2 m, and for λ_S ranging 24-2000 m every 32 m. That cost is not due to the computation of Equation 1, but to the smoothing of curvature for various λ_S.

Our study illustrates the valuable contribution of spatial information for earthquake ground-motion and damage prediction and monitoring. The method described in Section 3.1 allows retrieving high-resolution DSM from satellite imagery at any area of the globe. This method requires only a few hours of work (including manual verification of the quality of the obtained surface model). However, two aspects still prevent the application of our methodology to rapid forecast. First, getting the satellite images for the surface model can require several days or weeks depending on those factors: accessibility of our institutions to those images, and the weather over the area affected by the earthquake. Therefore, we highly recommend elaborating the high-resolution topographic models without waiting for the occurrence of the earthquake in the areas of interest. Second, this study is based on a DSM (model of the reflective surface, above ground, but also above canopy and building roofs) and not on a DTM (terrain-only model). This means the presence of elevated forests and large buildings in the studied area can artificially induce fake high-frequency topographic amplification at some locations in the FSC map. For example, the dotted green circle on Figure 4a points out such artifact: a large U-shape building in Amatrice affects the FSC amplification, only at the smallest *S*-wavelengths (Figure 4c). For this reason,

this study does not investigate λ_S shorter than 232 m (below, the artifacts are getting stronger than amplification due to actual terrain). Those artifacts can easily be identified by eye: they are sharp and localized patches. Still we believe rapid and automatic forecast should imperatively use high-quality DTM only. Methods to derive DTM from DSM do exist, and we are currently testing their accuracy for including them in our methodology.

6. CONCLUSIONS

Through the FSC proxy computed on a high-resolution DSM provided by Pléiades satellite imagery, we observe a striking spatial correlation between topographic curvature and the locations of the greatest structural damages at Amatrice for the August 24th, 2016, earthquake in Central Italy. The damages in this small town show a strong variability at the hectometric scale. Indeed the vulnerability of old buildings has a clear dominant role in the damage pattern. Nevertheless, we find that the spatial variability of the topographic site amplification, as predicted by FSC, also correlates with the spatial variability of the damages, on the same hectometric scale.
We relate smoothed-curvature maps with various ranges of affected *S*-wavelengths, emphasizing the level of FSC amplification reached at different spatial scales. The largest FSC amplification is reached at *S*-wavelengths ranging 200-900 m in the Northwestern part of the city. This indicates that the small topographic features (narrower than 500 m) are the ones most contributing to the topographic site effect over this hill, compared to larger scales. This study emphasizes the need to consider small scales and high-resolution models for investigating the local origins of earthquake damages. To this end, using spatial information (for topographic models and damage patterns) in our methodology proved to be much valuable. Thanks to that newly available information at high resolution, the small scales involved are now reachable for site-effect analyses.

Due to the double correlation of damages with vulnerability and topographic curvature, the link between earthquake damage and topographic amplification at Amatrice remains to some extent elusive. One interesting viewpoint that, to our opinion, deserves to be analyzed in future studies is what we call the "promontory effect". We observe that many ancient villages in the Apennines are located on top of hills or ridges, not necessarily much elevated (like Amatrice's hill), but with a pronounced curvature and steep slopes. There are several potential reasons for one village to be built on such configuration, depending on the period of construction. Those reasons may relate to military concerns (defensibility), to natural hazards (avoiding flood exposure), or to farming considerations (freeing the flat and irrigated valleys for farm fields). That typical settlement of ancient villages, gathering many buildings in a small and elevated area, is not only found in the Apennines: that is also a common feature in the mountainous environment along the French and Italian Riviera. As those villages combine the aggravating factors of high vulnerability and topographic amplification, and as they are located in seismically active regions, the promontory effect should be better understood and systematically identified. For example, it could be tested following the Viewshed analysis available in mapping tools.

Additionally to the propositions given in Section 5 within the scope of rapid application of our methodology for future earthquakes in mountainous areas, further works will consist in:
(1) Investigating with the same methodology the other villages affected by the Amatrice earthquake and located on hills or steep slopes: for examples, Pescara del Tronto (where topographic scales down to decametric could be involved), Accumoli, Arquata del Tronto and Saletta, among others.
(2) Performing 3D numerical simulations of earthquake ground motion to analyze potential interactions between finite-fault source and topography. Amatrice is indeed located in the near field of the seismic source and may have suffered a complex incident motion in the high frequencies. All past studies of the topographic site effect were performed either with synthetic considering a point source, or with recordings of aftershocks or small earthquakes. Yet the far-field hypothesis is certainly not applicable to the case of Amatrice. 3D numerical simulations will help to understand the coupling between the radiation from the extended source and the pronounced topography of the Apennines. One particular question is how far is the actual motion from the median motion predicted by the FSC proxy due to that near-field aspect?

(3) Considering, conjointly with the topography, the local site conditions at Amatrice. Effects of near-surface geology and heterogeneities cannot be excluded in that location, they may even be stronger than the effect of surface topography. The FSC proxy is currently not able to evaluate the relative contributions of all involved topographic and lithological effects. This study does not exclude that the inner geology of the hill could also have played a significant role in the distribution of damages. The FSC proxy is only valid in homogeneous medium, an assumption that can be very different from the actual situation at Amatrice. Further theoretical works are required to understand how site effects of different origins combine at the same location, and how the topographic amplification function is modified by heterogeneous medium. Once those interactions are better understood, the FSC proxy will have to be modified to become valid in heterogeneous medium, or another solution will be to combine it with other proxies of the effects of impedance contrasts at the near surface. This is a long-term task, for which both intensive numerical simulations of the ground motion and dense recordings of the involved phenomena are required. Concerning Amatrice, since the mainshock, many geophysical and geotechnical investigations were performed over the hill by several Italian institutions, in order to know its inner structure and the related site effects (however, some techniques are difficult to apply due to the narrow topography and results may be affected by large uncertainties).
(4) Crossing our results with improved vulnerability studies (e.g. Fiorentino et al. 2017) and with site-effect analyses based on actual recordings of the numerous aftershocks and ambient noise (e.g. Grelle et al. 2018), in order to fully understand the distribution of damages in Amatrice. The characteristics of the damaged *vs.* unaffected buildings are one important parameter of the problem, maybe the most important. This parameter must be included in our study in order to validate the potential of our rapid approach. Our results illustrate the small spatial scales involved in the problem, and therefore, we conclude that the vulnerability parameter must be available at the scale of each individual building. However, to our knowledge, that information is not publically available at Amatrice. As for the aftershock recordings performed at Amatrice, these data could allow us to compare the outcome of the FSC proxy with the actual amplification functions recorded over the hill. In particular, this comparison will provide information on the relative contributions of the involved topographic and lithological effects.
(5) At last, the FSC proxy will benefit from further developments based on a new bank of synthetic waveforms computed with up-to-date 3D numerical simulations. For example, it could be improved to take into account the back-azimuthal dependence of the topographic site effect. Currently the proxy gives statistical estimates of that dependence, but it is not able to predict the exact level of amplification for one given hypocenter related to the investigated area. Such improvement could allow taking into account extended fault instead of point source, and distinguishing which horizontal component of the ground motion is the most amplified by the topography.

7. ACKNOWLEDGMENTS

We thank ISIS program from CNES (French national agency for space studies) for providing access to the Pléiades satellite images.
This study uses products from the "Copernicus Emergency Management Service*"*, Directorate Space, Security and Migration, European Commission Joint Research Centre (EC JRC). The grading map shown in this study and the associated vector data are from activation ID EMSR177 (title: Amatrice aerial), last accessed November 28, 2017, http://emergency.copernicus.eu/.

8. REFERENCES

Assimaki D, Gazetas G, Kausel E (2005). Effects of local soil conditions on the topographic aggravation of seismic motion: parametric investigation and recorded field evidence from the 1999 Athens earthquake. *Bull. Seism. Soc. Am.*, 95: 1059-1089.

Berthier E, Vincent C, Magnússon E, Gunnlaugsson A, Pitte P, Le Meur E, Masiokas M, Ruiz L, Pálsson F., Belart JMC, Wagnon P (2014). Glacier topography and elevation changes derived from Pléiades sub-meter stereo images. *Cryosphere*, 8(6): 2275-2291.

Buech F, Davies TR, Pettinga JR (2010). The Little Red hill seismic experimental study: topographic effects on ground motion at a bedrock-dominated mountain edifice. *Bull. Seism. Soc. Am.*, 100(5A): 2219–2229.

Burjánek J, Edwards B, Fäh D (2014). Empirical evidence of local seismic effects at sites with pronounced topography: a systematic approach. *Geophys. J. Int.*, 197(1): 608–619.

Fiorentino G, Forte A, Pagano E, Sabetta F, Baggio C, Lavorato D, Nuti C, Santini S (2017). Damage patterns in the town of Amatrice after August 24th 2016 Central Italy earthquakes. *Bull. Earthq. Eng.*, published online.

Grelle G, Bonito L, Revellino P, Sappa G (2016). Frequency-dependent topographic seismic amplification by a "gray box model" using GIS morphometric data. *Rend. Online Soc. Geol. It.*, 41: 342-345.

Grelle G, Wood C, Bonito L, Sappa G, Revellino P, Rahimi S, Guadagno FM (2017). A reliable computerized litho-morphometric model for development of 3D maps of Topographic Aggravation Factor (TAF): the cases of East Mountain (Utah, USA) and Port au Prince (Haiti). *Bull. Earthq. Eng.*, published online.

Grelle G, Bonito L, Maresca R, Maufroy E, Revellino P, Sappa G, Guadagno FM (2018). The role of topographic effects on Amatrice's hill detected by SiSeRHMap and endorsed by experimental data and damage distribution. *16th European Conference on Earthquake Engineering*, Thessaloniki, Greece, June 18-21, extended abstract.

Hough SE, Altidor JR, Anglade D, Given D, Guillard Janvier M, Zebulon Maharrey J, Meremonte M, Bernard Saint-Louis M, Prepetit C, Yong A (2010). Localized damage caused by topographic amplification during the 2010 M7.0 Haiti earthquake. *Nat. Geosci.*, 3(11): 778–782.

Kawase H, Aki K (1990). Topography effect at the critical SV-wave incidence: possible explanation of damage pattern by the Whittier Narrows, California, earthquake of 1 October 1987. *Bull. Seism. Soc. Am.*, 80: 1–22.

Lacroix P, Berthier E, Taipe Maquerhua E (2015). Earthquake-driven acceleration of slow-moving landslides in the Colca valley, Peru, detected from Pléiades images. *Remote Sens. Environ.*, 165: 148-158.

Lacroix P (2016). Landslides triggered by the Gorkha earthquake in the Langtang valley, volumes and initiation processes. *Earth, Planets and Space*, 68(1): 1-10.

Maufroy E, Cruz-Atienza VM, Gaffet S (2012). A robust method for assessing 3-D topographic site effects: a case study at the LSBB Underground Laboratory, France. *Earthquake Spectra*, 28(3): 1097-1115. DOI: 10.1193/1.4000050

Maufroy E, Cruz-Atienza VM, Cotton F, Gaffet S (2015a). Frequency-scaled curvature as a proxy for topographic site-effect amplification and ground-motion variability. *Bull. Seism. Soc. Am.*, 105(1): 354-367. DOI: 10.1785/0120140089

Maufroy E, Perron V, Hollender F, Langlais M, Cruz-Atienza VM, Cotton F (2015b). Evaluation of topographic rock sites as reference sites, southeastern France: application of the Frequency-Scaled Curvature proxy. *Poster presented at the Seismological Society of America annual meeting*, 21-23 April, Pasadena, California.

Pischiutta M, Cultrera G, Caserta A, Luzi L, Rovelli A (2010). Topographic effects on the hill of Nocera Umbra, central Italy. *Geophys. J. Int.*, 182(2): 977–987.

Pischiutta M, Akinci A, Malagnini L, Herrero A (2016). Characteristics of the strong ground motion from the 24th August 2016 Amatrice earthquake. *Annals of Geophysics* 59, Fast Track 5.

Rai M, Rodriguez-Marek A, Asimaki D (2016). Topographic proxies from 2-D numerical analyses. *Bull. Earthq. Eng.*, 14(11): 2959-2975.

Rai M, Rodriguez-Marek A, Chiou BS (2017). Empirical terrain-based topographic modification factors for use in ground motion prediction. *Earthq. Spectra*, 33(1): 157-177.

Shean DE, Alexandrov O, Moratto ZM, Smith BE, Joughin IR, Porter C, Morin P (2016). An automated, open-source pipeline for mass production of digital elevation models (DEMs) from very-high-resolution commercial stereo satellite imagery. *ISPRS Journal of Photogrammetry and Remote Sensing*, 116: 101-117.

Spudich P, Hellweg M, Lee WHK (1996). Directional topographic site response at Tarzana observed in aftershocks of the 1994 Northridge, California, earthquake: implications for mainshock motions. *Bull. Seism. Soc. Am.*, 86(1B): S193-S208.

Stolte AC, Cox BR, Lee RC (2017). An experimental topographic amplification study at Los Alamos National Laboratory using ambient vibrations. *Bull. Seism. Soc. Am.*, 107(3): 1386-1401.

Tinti E, Scognamiglio L, Michelini A, Cocco M (2016). Slip heterogeneity and directivity of the M_L 6.0, 2016, Amatrice earthquake estimated with rapid finite-fault inversion. *Geophys. Res. Lett.* 43(20): 10,745-10,752.